PHYSICAL REVIEW E, VOLUME 64, 020901(R)

All-optical measurements of the bending rigidity of lipid-vesicle membranes across structural phase transitions

Chau-Hwang Lee,[1,*] Wan-Chen Lin,[1] and Jyhpyng Wang[2,3]
[1]*Institute of Applied Science and Engineering Research, Academia Sinica, Taipei 115, Taiwan*
[2]*Institute of Atomic and Molecular Sciences, Academia Sinica, Taipei 106, Taiwan*
[3]*Institute of Electro-Optical Engineering, National Taiwan University, Taipei 106, Taiwan*
(Received 19 January 2001; revised manuscript received 4 May 2001; published 23 July 2001)

By exploiting the nanometer sensitivity of the confocal response to the position of an in-focus reflecting surface, we measured the bending rigidity of lipid-bilayer vesicles with a noninvasive all-optical method. The vesicles were weakly deformed with femtonewton optical force, and the bending rigidity was measured continuously from the L_α through the $P_{\beta'}$ to the $L_{\beta'}$ phases on the same specimen for the first time. The bending modulus is found to increase by an order of magnitude from the L_α phase to the $L_{\beta'}$ phase, as a result of the increasing area-compressibility modulus and bilayer thickness. The dips of bending modulus give precisely the main-transition and pretransition temperatures, which supports the recently proposed chain-melting model of pretransition.

DOI: 10.1103/PhysRevE.64.020901 PACS number(s): 87.16.Dg, 87.15.La, 87.64.−t

Lipid vesicles have attracted much interest as an idealized model system in biophysics research. They not only serve as simple models for gaining insight into real biomembranes, but also hold the promise of important medical applications, such as controlled drug delivery [1]. A subject of considerable interest in lipid vesicle research is the mechanical and thermodynamical properties of vesicle membranes. In the past two decades, several methods for studying these properties have been developed. Microscopic methods include neutron diffraction [2], x-ray diffraction [3], and electron-spin resonance [4]; whereas macroscopic methods include differential scanning calorimetry [3], the micropipette method [5–7], spectral analysis of shape fluctuations [8–10], atomic force microscopy [11], and optical dynamometry [12]. Microscopic methods provide structural data at the molecular level, yet numerical modeling or molecular dynamics simulations are required to relate these data to macroscopic properties [13]. Macroscopic methods offer more direct measurements on membrane response to external perturbations, but contact methods are mostly invasive, which may drive the specimen out of its natural state. For example, large bending of bilayer membranes can lead to lipid exchange between the two monolayers [7]. On the other hand, pure optical methods are so far limited by resolution. For example, spectral analysis of shape fluctuations is an elegant noninvasive optical method, but for lipid vesicles in the gel phase the fluctuations are in the nanometer range, too small to be resolved by conventional optical microscopy. Optical dynamometry has been successfully applied to large vesicles (radii $>40\ \mu$m), but it cannot be applied to much smaller ones because data interpretation requires that the beads sit on a flat surface. Atomic force microscopy is a powerful method for studying the viscoelastic properties of soft condensed matters, e.g., supported lipid bilayers [11] and living cells [14,15], with resolution down to a few nanometers. However, the application of atomic force microscopy to unsupported bilayer membranes was not successful because of membrane damage by the probe. To circumvent these limitations and concerns, a general purpose, noninvasive, high resolution and all-optical method is much desired.

A fundamental macroscopic property of lipid bilayers is the bending rigidity, which is closely related to the shape, stability, strength, and structural phases. Quantitative study of bending rigidity in different phases is also important for the applications [16]. The macroscopic methods mentioned above have all been employed to study the bending rigidity. In the micropipette methods, the bending rigidity is derived from the slope of the logarithmic function of surface tension versus the area dilation, under the assumptions of uniform tension and symmetric bilayers without spontaneous curvature effects [6]. The two assumptions are known to be both valid only for the fluid (L_α) phase; therefore, this method has not been applied to membranes in the gel state. The method of spectral analysis of shape fluctuations uses conventional optical microscopy to observe the deformation, but because the deformation is driven by thermal fluctuations, this method is applicable only for the well-deformable L_α phase [8,9,17,18]. Measurements for the rippled ($P_{\beta'}$) phase are even more complicated and model-dependent. For the micropipette method, bending rigidity is estimated from the area compressibility modulus K_a and the amplitude of the surface ripples measured by x-ray diffraction [5]. Because these two parameters cannot be measured for the same specimen, this method has limited accuracy. In two-bead optical dynamometry [12], membrane elastic stiffness η in the $P_{\beta'}$ phase is measured and then translated into the bending modulus κ through a linear relation: $\eta \approx C\kappa/\delta^2$, where δ is the bead radius and C is an empirical proportional constant. But this method cannot be applied to bilayers in the L_α phase because η does not exist for fluid bilayers. Moreover, the proportional constant C is determined from measurements of large systems (such as a rubber sheet), whether the same

*Corresponding author. FAX: 886-2-2782-6680. Email address: clee@gate.sinica.edu.tw

 ©2001 The American Physical Society

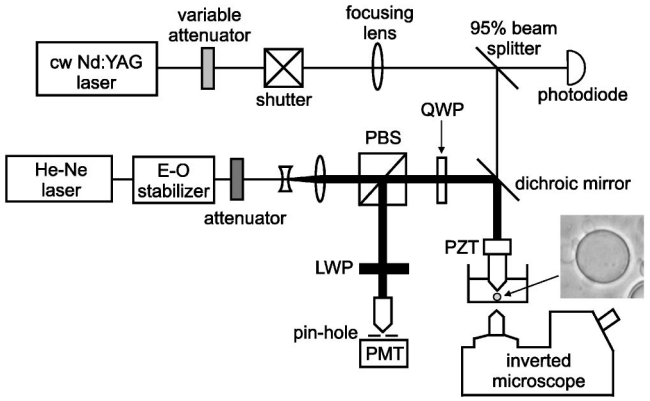

FIG. 1. Experimental setup. LWP, long-wavelength-pass filter; PBS, polarization beam splitter; PMT, photo-multiplier tube; PZT, piezoelectric transducer; QWP, quarter wave plate. Inset: phase-contrast image of a DPPC bilayer vesicle.

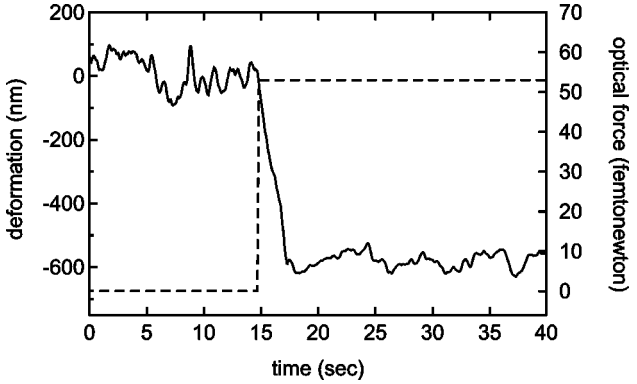

FIG. 2. DPPC vesicle deformation along the optical axis under 53-femtonewton optical force at 30 °C. The original diameter of this vesicle is 15 μm. Solid line, membrane deformation; dashed line, optical force.

value can be applied to vesicles is still an open question, owing to the lack of an appropriate theory [12]. As to the gel ($L_{\beta'}$) phase, no method of measuring the bending rigidity has been reported yet.

In this Rapid Communication we developed an all-optical method for measuring the bending rigidity of lipid bilayers across all phases. Bending rigidity was studied by pressing the vesicle noninvasively with optical force and measuring its deformation directly with a nanometer-resolution optical technique. Data interpretation for such direct measurements does not rely on specific models; therefore, this method is suitable for bilayers in different phases. The temperature dependence of bending rigidity was measured continuously across the main transition and the pretransition on the same specimen by the same method. Nanometer resolution in the measurement of membrane deformation was achieved with the differential confocal technique [19]. In this technique the membrane is illuminated with a tightly focused low-power laser beam. When the membrane is placed slightly above or below the focal plane, the size and divergence of the reflected beam change sensitively with the distance between the membrane and the focal plane. By refocusing the retroreflected beam at a pin-hole spatial filter and measuring the transmitted power, the position of the membrane can be accurately determined. The technique is different from conventional confocal microscopy in that the surface is intentionally placed at a distance on the order of wavelength away from the focal plane, so that the sharp slopes of the confocal axial response curve are utilized to improve the depth resolution from $\sim\lambda$ to $\sim\lambda/300$. In contrast to interferometry, the differential confocal technique does not compare phases of different optical paths, therefore no servo-control on optical path length is needed. Simplicity makes the technique highly reliable and versatile.

The experimental setup is shown in Fig. 1. A 532-nm cw Nd:YAG laser (GCL-100-S, CrystaLaser) was used to apply the optical force on the vesicle, and a 633-nm He-Ne laser (25LHP151, Melles Griot) was used to measure the deformation. Both beams were focused on the vesicle membrane with a 40×, 0.75 N.A. water-immersion objective lens (ICS Achroplan, Carl Zeiss). The 532-nm beam was pre-focused on the entrance pupil of the objective lens, such that its diameter was 14 μm on the focal plane of the objective lens. The probe beam was expanded before entering the objective lens in order to be focused to a 1-μm diameter at the center of the 532-nm beam. Because the size of the 532-nm beam was much larger than the 633-nm beam, and its Rayleigh range is as large as 290 μm, the membrane deformation was measured under uniform optical pressure. The 633-nm probe light reflected from the vesicle membrane was filtered by a 5-μm diameter pin-hole at the conjugate focal point. The throughput was measured as the signal, which reached a maximum when the membrane was exactly at the focal plane. For the objective lens and the pin-hole we used, away from the focal plane by 1.2 μm the signal dropped to near zero. We intentionally placed the vesicle surface about 0.5 μm away from the focal plane to make the signal change sensitively with the membrane position. A 10-nm change of membrane position along the optical axis causes about 1% change of signal. We have used a similar setup to measure the viscoelastic susceptibility curves of living-cell membranes under different conditions of the cytoskeleton [20], and the potential of this technique for studying mechanical properties and morphology of lipid bilayers has been pointed out in Ref. [21].

Vesicles were prepared with the procedures described in Ref. [22]. We controlled the diameters of vesicles in the range of 10–20 μm by setting appropriate incubation temperatures. Phase-contrast microscopy [23] was used to verify that the vesicles were unilamellar. The inset in Fig. 1 shows a phase-contrast image of a typical dipalmitoyl phosphatidylcholine (DPPC) vesicle. As we turned on the 532-nm beam, the vesicle shape changed from a sphere to an oblate spheroid, with the top membrane shifting along the optical axis to a new equilibrium position, as shown in Fig. 2. The power of the 532-nm beam was 40 mW, and that of the probe beam was only 80 μW, both measured after the water-immersion objective lens. The power fluctuation of the probe beam was controlled by an electro-optical stabilizer (LS-PRO, CRI) to smaller than 0.02%. The bandwidth of the stabilizer was DC to 2 MHz, and the power fluctuation was measured in one minute using a 16-bit analog-to-digital converter at a 40-Hz

sampling rate. Because the membrane reflectivity was only 1.5×10^{-4}, the reflected probe-beam power on the photomultiplier tube was a few nanowatts. Therefore, we set the detection time constant to one second such that shot noise was less than 0.01%. Both the power fluctuation and the shot noise were controlled to be much smaller than the fluctuations of the vesicle membrane. In Fig. 2 the vesicle was found to be deformed by ~600 nm under 53-femtonewton force. The optical force was calculated from momentum conservation of the reflected photons. In a medium with refractive index n, the momentum of a photon is nh/λ, where h is Planck's constant [24]. For normal reflection on a surface with reflectivity R the optical force is thus $2nPR/c$, where P is the incident optical power and c is the speed of light in vacuum [25]. Because the absorption of lipid bilayers at the laser wavelengths is much smaller than reflection, we consider reflection as the only source of optical force. The change in membrane free energy was equal to the work done by the optical force, bending modulus was then derived directly from the energy conservation law.

Considering a vesicle surface Ω, the free energy E can be expressed as:

$$E=\frac{\kappa}{2}\int_{\Omega}(c_1+c_2)^2dA+\overline{\kappa}\int_{\Omega}c_1c_2dA, \tag{1}$$

where κ is the bending modulus, c_1 and c_2 are the principal curvatures of the membrane, dA is the surface element, and $\overline{\kappa}$ is the Gaussian rigidity [26]. For continuous perturbations of a closed surface, $\int_{\Omega}c_1c_2dA=4\pi$, independent of the principal curvatures [27]. In this case the change in free energy results only from the change of the first integral in Eq. (1). Therefore, once the values of $\int_{\Omega}(c_1+c_2)^2dA$ before and after the deformation are obtained, the value of κ can be determined. Before the deformation no external stress is applied on the membrane, and a unilamellar lipid vesicle forms an almost perfect sphere [28], such that $c_{o1}=c_{o2}=-1/r_0$, where r_0 is the original radius of the vesicle. In this case we have $E=8\pi\kappa+4\pi\overline{\kappa}$. While the vesicle is deformed along the optical axis, its shape becomes an oblate spheroid with the length of the short axis $2a$ and that of the long axes $2b$. In our experiments the change in diameter was within 4–11 % when the vesicle was deformed, which means the optical force and the supporting force from the bottom are only small perturbations compared with the surface tension. Therefore, an oblate spheroid is a good approximation. The volume of the vesicle can change during the deformation because of the suspected pore formation at the transition point [29]. In contrast, because the area compressibility modulus of lipid bilayers is as large as 10^{-10} newton/nm [5,30], the femtonewton optical force cannot change the surface area. Therefore the constant-surface-area constraint instead of the constant-volume constraint should be used to determine b from the measured value of a. In practice, in our experiments the deformation was so small that the difference in b calculated from the two constraints is smaller than 0.2% of the vesicle diameter. This is smaller than the uncertainty of the measurements, which is 0.6% of the vesicle diameter.

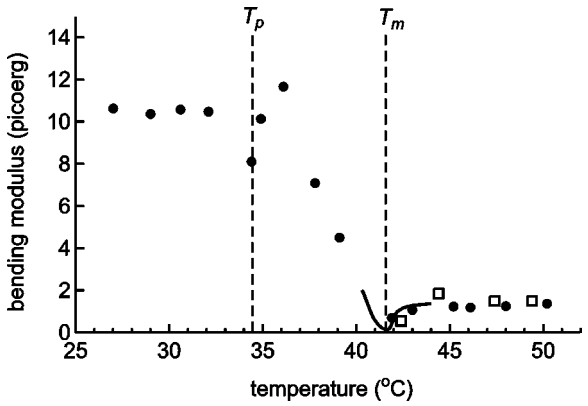

FIG. 3. Bending modulus of a DPPC vesicle bilayer as a function of temperature. Closed circles, data measured in this work; open squares, data measured in Ref. [17]. Solid curve, estimation in Ref. [32].

The principal curvatures of an oblate spheroid are [31]

$$c_{d1}=-\frac{r^2-r(d^2r/d\theta^2)+2(dr/d\theta)^2}{[r^2+(dr/d\theta)^2]^{3/2}}, \tag{2}$$

and

$$c_{d2}=-\frac{2r^2}{b^2[4r^2+r^{-2}(dr^2/d\theta)^2]^{1/2}}, \tag{3}$$

where θ is the azimuthal angle of the surface element from the short axis, and $r(\theta)=ab/(a^2\sin^2\theta+b^2\cos^2\theta)^{1/2}$. The bending modulus κ can then be directly calculated with the following equation:

$$\kappa=\frac{2W}{\int_{\Omega}(c_{d1}+c_{d2})^2dA-16\pi}, \tag{4}$$

where W is the work done by the optical force. To check the reliability of our method, we compare our data with previously established methods. We used the bending moduli of the dimyristoyl phosphatidylcholine (DMPC) bilayer vesicle in the fluid phase for the comparison because for this sample more data are available in the literature. For DMPC we measured $\kappa=1.41\pm0.13$ picoergs at 27 °C and 1.33 ± 0.12 picoergs at 30 °C. With spectral analysis of shape fluctuations, κ of DMPC was measured to be 1.52 ± 0.06 picoergs at 27 °C and 1.30 ± 0.08 picoergs at 30 °C [18]. No discrepancy was found between the two measurements.

For studying phase transitions, DPPC is more convenient because of its higher transition temperatures. In Fig. 3, we show the bending moduli of a DPPC bilayer measured from 50 °C down to 27 °C. The temperature accuracy was ±0.1 °C. The temperature was varied with a gradient of -0.2 °C/min, and at each temperature stop the temperature was maintained for one hour for shape relaxation before the measurement. Because the diameter of the vesicle changed as the temperature was varied, at each temperature we mea-

sured the individual diameter and deformation of the vesicle, then calculated κ with the procedure described above. The bending modulus as a function of temperature makes two clear dips exactly at the pretransition temperature T_p and the main-transition temperature T_m previously measured by differential scanning calorimetry [32]. This is in agreement with the recently proposed chain-melting model of pretransition [33]. In the L_α phase ($T>T_m$) where previous measurements are available [17], the data also compares well, as shown by the open squares in Fig. 3. In the $P_{\beta'}$ phase ($T_m>T>T_p$), κ increases monotonically as the temperature is decreased. From 41.9 °C to 36.1 °C κ increases by more than an order of magnitude. This trend agrees with the estimation of κ in the $P_{\beta'}$ phase from the specific heat of the bilayer [32], and is consistent with optical dynamometry study on DMPC bilayers [12]. Below T_p the bilayer is in the $L_{\beta'}$ phase and κ becomes insensitive to the temperature. We measured κ of over 30 DPPC vesicles, and the results in Fig. 3 are typical values. From vesicle to vesicle the variation of κ is $\pm 8.5\%$.

The near tenfold increase of bending modulus from the L_α phase to the $L_{\beta'}$ phase is an interesting result. According to the classical elasticity theory, for an isotropic bilayer with symmetric and decoupled monolayers, the bending modulus κ scales with the area compressibility modulus K_a and the bilayer thickness l according to the following equation [13,34]:

$$\kappa \propto K_a l^2. \tag{5}$$

Equation (5) is good for calculating κ in the limit of small curvature [32], such as the case in this work. When the DPPC membrane makes transition from the L_α phase to the $L_{\beta'}$ phase, K_a has been measured to increase by 6.9 folds and l by 1.3 folds [30]. Combining these two factors, Eq. (5) suggests that the bending modulus of DPPC bilayers increases by 11.7 folds from L_α phase to $L_{\beta'}$ phase. This is indeed observed in our measurements. The interesting part is that Eq. (5) was only known previously to work for the L_α phase [17,32], and in the gel phase the coupling between the two monolayers has been suspected to make this scaling law invalid [32]. It was not possible to check its validity for the gel phase owing to the lack of measurement techniques. Our measurements indicate that the coupling between the two monolayers is not an important effect, at least when the curvature of the bilayer is small.

In summary, we have developed an all-optical method to detect the structural phase transitions and to determine the bending rigidity of lipid bilayers. The difficulty of measuring sub-micrometer deformation on the less deformable gel state is overcome with the differential confocal technique. After the weak perturbation of optical force, the vesicle returns to its natural shape; therefore, we could repeat the measurement on the same vesicle while changing ambient conditions continuously. The same measurement procedures can be applied to various kinds of soft condensed matters, such as lipid tubules, polymersomes [35], etc. Thanks to the high resolution and long working distance of the differential confocal technique, the samples can be measured *in situ*, with straightforward data interpretation. The high spatial resolution and real-time capability can also be utilized to explore dynamic properties of vesicles, such as budding, fission, or fusion. We believe the method presented here can serve as a powerful general tool for the investigation of soft condensed matters in the micrometer scale.

[1] D. D. Lasic, *Liposomes: From Physics to Applications* (Elsevier, Amsterdam, 1993).
[2] G. Buldt *et al.*, Nature (London) **271**, 182 (1978).
[3] M. J. Janiak *et al.*, J. Biol. Chem. **254**, 6068 (1979).
[4] K. Tsuchida and I. Hatta, Biochim. Biophys. Acta **945**, 73 (1988).
[5] D. Needham and E. Evans, Biochemistry **27**, 8261 (1988).
[6] E. Evans and W. Rawicz, Phys. Rev. Lett. **64**, 2094 (1990).
[7] D. V. Zhelev *et al.*, Biophys. J. **67**, 720 (1994).
[8] H. P. Duwe *et al.*, J. Phys. (France) **51**, 945 (1990).
[9] M. D. Mitov *et al.*, in *Advances in Supramolecular Chemistry*, edited by G. W. Gokel (JAI Press, Greenwich, 1992), Vol. 2, pp. 93–139.
[10] A. Zilker *et al.*, Phys. Rev. A **46**, 7998 (1992).
[11] Z. Shao and J. Yang, Q. Rev. Biophys. **28**, 195 (1995).
[12] R. Dimova *et al.*, Biophys. J. **79**, 340 (2000).
[13] R. Goetz *et al.*, Phys. Rev. Lett. **82**, 221 (1999).
[14] H. C. van der Mei *et al.*, Biophys. J. **78**, 2668 (2000).
[15] R. E. Mahaffy *et al.*, Phys. Rev. Lett. **85**, 880 (2000).
[16] B. A. I. van den Bergh *et al.*, J. Controlled Release **62**, 367 (1999).
[17] L. Fernandez-Puente *et al.*, Europhys. Lett. **28**, 181 (1994).
[18] P. Méléard *et al.*, Biophys. J. **72**, 2616 (1997).
[19] C.-H. Lee and J. Wang, Opt. Commun. **135**, 233 (1997).
[20] C.-H. Lee, C.-L. Guo, and J. Wang, Opt. Lett. **23**, 307 (1998).
[21] C.-M. Chen, Phys. Rev. E **59**, 6192 (1999).
[22] K. Akashi *et al.*, Biophys. J. **71**, 3242 (1996).
[23] R. M. Servuss and E. Boroske, Phys. Lett. **69A**, 468 (1979).
[24] R. V. Jones and B. Leslie, Proc. R. Soc. London, Ser. A **360**, 347 (1978).
[25] E. Hecht, *Optics*, 2nd ed. (Addison-Wesley, Reading, 1987), Sec. 3.3.
[26] W. Helfrich, Z. Naturforsch. C **28**, 693 (1973).
[27] H. J. Deuling and W. Helfrich, Biophys. J. **16**, 861 (1976).
[28] M. Abkarian *et al.*, Phys. Rev. E **63**, 041906 (2001).
[29] L. A. Bagatolli and E. Gratton, Biophys. J. **77**, 2090 (1999).
[30] R. P. Rand and V. A. Parsegian, Biochim. Biophys. Acta **988**, 351 (1989).
[31] See, e.g., I. S. Sokolnikoff, *Tensor Analysis: Theory and Applications to Geometry and Mechanics of Continua*, 2nd ed. (John Wiley & Sons, New York, 1964), Sec. 72.
[32] T. Heimburg, Biochim. Biophys. Acta **1415**, 147 (1998).
[33] T. Heimburg, Biophys. J. **78**, 1154 (2000).
[34] E. Evans, Biophys. J. **14**, 923 (1974).
[35] B. M. Disher *et al.*, Science **284**, 1143 (1999).